PART ONE: INTRODUCTION, BACKGROUND AND LITERATURE REVIEW

1. INTRODUCTION AND BACKGROUND

Nickel-based superalloys have excellent mechanical properties because they have a microstructure comprising many small, strained-coherent, particles in a softer matrix [1987Sim]. The strengthening originates from dislocations being slowed down as they negotiate the small ordered particles. Additionally, there is solid solution strengthening in the (Ni) matrix. Although these alloys are used at relatively high temperatures, coarsening does not occur because the surface energy itself is very small. This is because the particle structure is very closely related to that of the matrix. Both are based on the face centred cubic structure: the matrix has a random fcc structure, and the particles have an $L1_2$ ordered structure (ordered fcc). Thus, the lattice misfit between these structures is very small and renders the surface energy negligible [1987Sim].

The Ni-based superalloys have virtually reached their temperature limit for operation in turbine engines. However, there is a need to further increase the operational temperatures of these engines to achieve greater thrust, reduced fuel consumption and lower pollution. Thus, there is interest in developing a whole new suite of similar structured alloys based on a metal with higher melting point which can be used at temperatures of ~1300^{o}C.

Platinum has been selected as the base material for these alloys because of its similarity to Ni in fcc structure and similar chemistry. Thus, similar phases to Ni_3Al could be used to give similar mechanisms as found in the Ni-based superalloys. The important differences are the higher melting point (1769^{o}C for platinum compared to 1455^{o}C for nickel) and improved corrosion resistance. These facts inspired the proposal by Wolff in 2000 that Pt-based analogues to Ni superalloys could be developed to serve in the most critical and demanding of high temperature applications [2000Wol]. Although Pt-based alloys are unlikely to replace all Ni-based superalloys because of their higher price and higher density, it is likely that they can be used for the highest temperature components. Pt_3Al has two forms, and the more desirable high temperature cubic $L1_2$ form needs to be stabilised, rather than the tetragonal DO'_c form.

Experimental Pt-based alloys have been studied. It was found that successful Ni-based superalloy analogues could be manufactured with alloys of the approximate composition $Pt_{82}:Al_{14}:X_4$ where X was Cr, Ti and Ru [2001Hil1, 2001Hil2]. The best properties were exhibited by the Pt-Al-Cr and Pt-Al-Ru alloys, although the precipitate volume fraction was not as high as in the Ni-based superalloys. Although much heavier, the Pt-based alloys have the advantages of good mechanical properties and high temperature oxidation resistance [2000Hil, 2001Süs1]. The ternary alloys have mechanical properties which are better than those of the Ni- and Co-based superalloys, higher than conventional solid-solution strengthened Pt-based alloys, and comparable with mechanically alloyed ferritic ODS alloys [2002Süs1].

As has been shown before [2001Hil3], it is possible to obtain a (Pt) + ~Pt_3Al microstructure in the quaternary alloys. The volume fraction of ~Pt_3Al was estimated, using image analysis, to be approximately 25-30%. The highest hardness was found in the alloy without primary ~Pt_3Al. In the second batch of quaternary alloys, there was no clear relationship between the hardness and the composition or microstructure. The decrease in hardness after the second heat treatment is likely to be due to the changes in composition due to oxidation. Several alloys were made up in order to ascertain whether the two-phase structure could be achieved in the quaternary system [2002Cor1]. Compositions were selected based on the results of the ternary Pt-Al-Cr and Pt-Al-Ru systems. It was shown that it is possible to produce a fine two-phase γ/γ' structure in the Pt-Al-Ru-Cr system, with precipitates of similar shape to those in the nickel-based superalloy systems. Oxidation tests have shown that the quaternary system has favourable high temperature oxidation resistance [2001Süs2]. The composition of $Pt_{84}:Al_{11}:Ru_2:Cr_3$ is the optimum composition because it has no primary phase.

Work has been ongoing in building a thermodynamic database for the prediction of phase equilibria in these Pt-based superalloys that are being developed. The database will aid the design of alloys by enabling the calculation of the composition and proportions of phases present in alloys of different compositions. This will save both time and money. At minimum, the database should comprise Pt, Al, Cr and Ru.

The work is being done using the Thermo-Calc^{TM} software, and the database is being built up by obtaining good thermodynamic descriptions of all of the possible phases in the system. The Parrot module in Thermo-Calc^{TM} [1985Sun] is being used to optimise the database that is based on that of the SGTE group [1991Din] and Spencer's database [1998Spe]. The supplied database did not cover all of the phases, and these had to be gleaned from literature, or modelled using experimental data. Similarly, not all of the experimental data were known, and where there are gaps or inconsistencies, experiments have to be undertaken. Selected important binaries were optimised first, for example, Al-Ru [2003Pri] and Al-Pt [2002Pri1]. Once each binary system is modelled satisfactorily, they can be added into the ternary systems, after which each ternary system must be optimised individually. This is done using the experimental data gleaned either from literature, or, as was mostly the case, derived experimentally at the University of the Witwatersrand and Mintek. Experimental phase diagram work was completed on the ternary systems: Al-Cr-Ru [2000Com1, 2000Com2, 2001Com], Pt-Al-Ru [2002Pri2, 2005Pri] and Pt-Cr-Ru [2002Süs1, 2003Süs1, 2003Süs2, 2004Süs1, 2006Süs1]. The Pt-Al-Cr system was the last remaining system that needed to be studied, with some preliminary work that had been done [2003Süs3].

A preliminary version of the database was constructed from assessed thermodynamic datasets for the binary systems only. The binary descriptions were combined allowing extrapolation into the ternary systems and experimental phase equilibrium data were compared with calculated results. Very good agreement was obtained for the Pt-Al-Ru [2003Pri, 2004Pri] and reasonable agreement for the Pt-Cr-Ru [2004Süs2] system, which was encouraging and confirmed that the higher order systems could be calculated from the binary systems with confidence. Since some of the phase models in databases were different, these phases have to be remodelled. However, more work is ongoing for information concerning the ternary phases present in the Al-Cr-Ru and Pt-Al-Ru systems (two ternary compounds in each).

Since limited research has been done on Pt-based alloys, and the phase diagram work has been poorly documented, this project will vastly extend the knowledge base of Pt systems. This work will ultimately expand to Pt alloys of higher order. There is already collaboration with the University of Bayreuth and Fachhochschule Jena, Germany, to expand the experimental work and thermodynamic the database to include nickel, as well as cobalt. The extension of the Pt systems knowledge base might encourage incorporation of Pt into other alloy systems.

This thesis follows on the M.Sc. dissertation [2004Süs1] as part of the phase diagram work necessary for the development of a thermodynamic database for the quaternary Pt-Al-Cr-Ru system. Whereas the M.Sc. dissertation only focussed on experimental work, this thesis focuses primarily on the results of the experimentally determined phase equilibria in the Pt-Al-Cr system, but also includes results on the thermodynamic modelling of Pt-Cr-Ru and particularly Pt-Al-Cr.

2. LITERATURE REVIEW

No work has been published before on the Pt-Al-Cr ternary system by investigators outside of Mintek. A clear understanding of the binary systems which constitute the ternary systems is therefore important. These are: Pt-Cr, Pt-Al and Al-Cr. These are addressed in the following section, and will include information pertaining to both experimental work as well as thermodynamic modelling. Results by Hill [2001Hil4] from earlier work done at Mintek on the Pt-Al-Cr system will also be presented.

2.1. The binary Cr-Pt phase diagram

Venkatraman and Neumann [1990Ven] reviewed the Cr-Pt system and their assessed diagram (Figure 1.1 [1990Mas]) is based primarily on the experimental work by Müller [1930Mül] and Waterstrat [1973Wat]. Waterstrat [1973Wat] made an extensive study using microscopic, XRD and electron microprobe techniques [1973Wat]. More recently, Oikawa et al. gave a calculated phase diagram [2001Oik], and Zhao et al. proposed a refined version of the accepted diagram, based on thermal conductivity mapping [2005Zhao].

Solid Phases

Table 1.1 shows the solid phases and their crystal data.

Table 1.1. Solid phases of Cr-Pt.

Phase/ Temperature Range (°C)	**Pearson Symbol/ Space Group/ Strukturbericht/ Prototype**	**Lattice Parameters (nm)**	**Comments**
(Cr) <1863	$cI2$ $Im\overline{3}m$ $A2$ W	a = 0.288	[1985Vil1]
Cr_3Pt <1600	$cP8$ $Pm\overline{3}n$ $A15$ Cr_3Si	a = 0.471	[1956Gre]
CrPt <700?	$tP4$ $P4/mmm$ $L1_0$ AuCu	a = 0.382 c = 0.381	[1976Bag]
CrPt <700?	$cF4$ $Fm\overline{3}m$ $A1$ *Cu*	a = 0.380	[1985Vil2]
CrPt <700?	$cP8$ $Pm\overline{3}n$ $A15$ Cr_3Si	a = 0.471	[1985Vil2]
$CrPt_3$ <1130	$cP4$ $Pm\overline{3}m$ $L1_2$ $AuCu_3$	a = 0.387	[1978Bag1]
(Pt) <1769	$cF4$ $Fm\overline{3}m$ $A1$ Cu	a = 0.392	[1985Vil3]

Phase Equilibria

Table 1.2 and Figure 1.1 show the phase equilibria. The liquidus and solidus points from 20 to 100 at.% Pt are taken from Müller and Waterstrat [1930Mül, 1973Wat]. They both found a maximum melting point of (Pt) at ~80 at.% at 1780°C and 1790°C respectively [1930Mül, 1973Wat]. Raub et al. [1955Rau] found that Cr_3Pt probably melts congruently and not syntectically as tentatively suggested by Waterstrat [1973Wat]. Both Raub and Waterstrat established the presence of a eutectic reaction on either side of Cr_3Pt [1930Mül, 1973Wat].

These eutectic temperatures were taken from Waterstrat [1973Wat], as well as the solid-state boundaries of (Cr), Cr_3Pt and (Pt). In agreement with previous studies [1930Mül, 1934Nem, 1935Fri, 1940Geb, 1955Rau, 1968Kus], it was observed that (Pt) had a broad solubility range (~29 to 100 at. %Pt at 1530°C) [1973Wat]. Several investigators showed that ordered fcc $CrPt_3$ forms from disordered (Pt) below 1200°C [1934Nem, 1935Fri, 1940Geb, 1955Rau, 1956Gre, 1962Bro, 1962Pic, 1963Pic, 1968Kus, 1973Wat]. The high temperature (Pt) phase can only be partially obtained by quenching [1935Fri, 1955Rau, 1968Kus, 1973Wat]. $CrPt_3$ remains cubic over its whole composition range from 50-85 at.% Pt [1935Fri, 1940Geb, 1955Rau, 1963Pic, 1973Bes, 1973Wat, 1977Got]. $L1_2$ $CrPt_3$ orders to an $L1_0$ type at composition CrPt without the tetragonal distortion typical of this structure [1963Pic, 1973Bes, 1973Wat, 1977Got]. Through thin-film studies, however, a tiny distortion as well as a CrPt/$CrPt_3$ two-phase region was shown [1977Bag, 1978Bag1, 1978Bag2]. More studies are required to resolve the latter two issues.

In the recent proposed refined version of the Pt-Cr diagram [2005Zhao], the two ordered phases (CrPt and $CrPt_3$) are shown in separate phase regions with the disordered fcc region between them (Figure 1.2), i.e. (Pt) the does not order to CrPt via $CrPt_3$, but fcc (Pt) orders to either CrPt or $CrPt_3$ depending on the composition. The new proposed phase diagram seems to be more sensible than the old one.

Oikawa et al. [2001Oik] calculated the diagram (Figure 1.3) with the relative temperatures of the eutectic reactions inverted compared to those in Figure 1.1 [1990Mas]. Süss et al. [2004Süs, 2005Süs, 2006Süs1] found that the only way to explain the microstructures, and hence reactions, in as-cast samples of Cr-Pt-Ru was that the relative eutectic temperatures agreed with Oikawa et al. and not Waterstrat. The same was found by Nzula et al. in as-cast samples of Cr-Ni-Pt [2005Nzu].

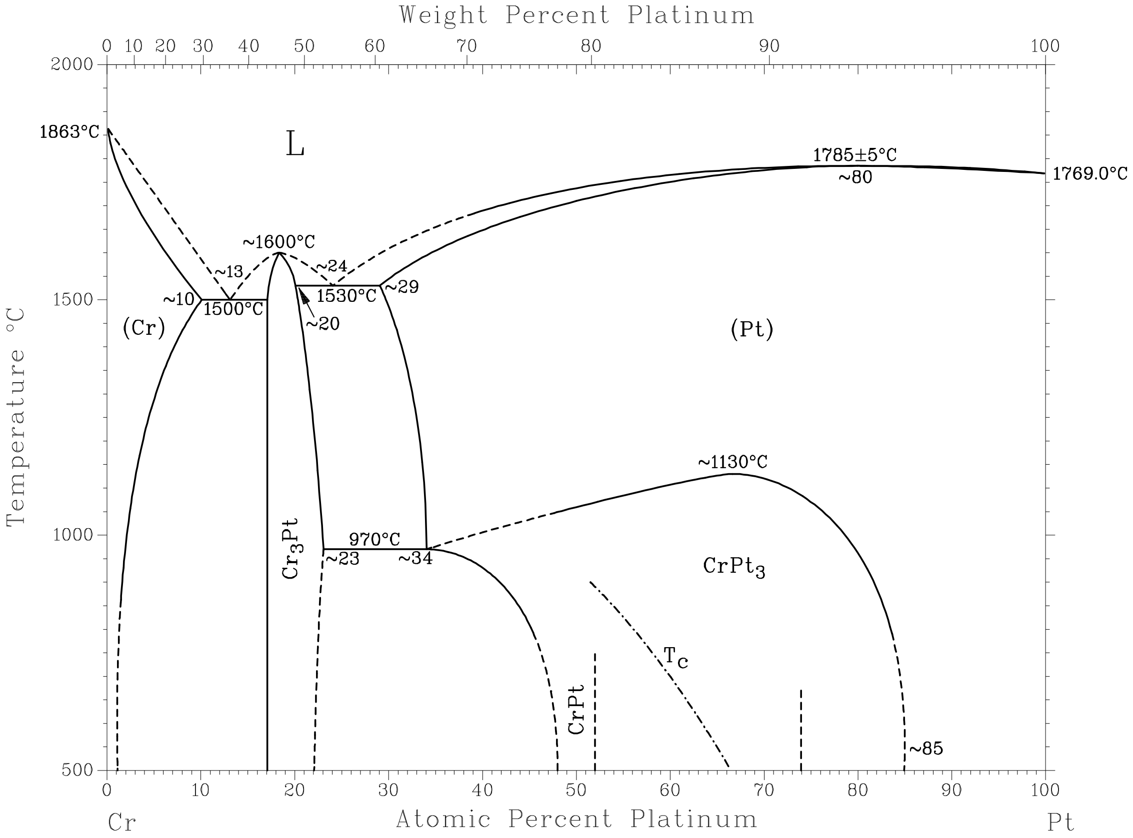

Figure 1.1. Binary Cr-Pt equilibrium phase diagram [1990Mas].

Table 1.2. Invariant equilibria of Cr-Pt.

Reaction	**T (°C)**	**Type**	**Phase**	**Composition (at.%)**	
				Cr	**Pt**
L → Cr_3Pt	~1600	Congruent	L Cr_3Pt	~82 ~82	~18 ~18
L → Cr_3Pt + (Pt)	1530	Eutectic	L Cr_3Pt (Pt)	~76 ~80 ~71	~24 ~20 ~29
L → (Cr) + Cr_3Pt	1500	Eutectic	L (Cr) Cr_3Pt	~87 ~90 ~83	~13 ~10 ~17
(Pt) → Cr_3Pt	~1130	Ordering	(Pt) Cr_3Pt	~33 ~33	~67 ~67
(Pt) → Cr_3Pt + $CrPt_3$	970	Eutectoid	(Pt) Cr_3Pt $CrPt_3$	~66 ~77 ?	~34 ~23 ?
L → (Pt)	1785±5	Congruent	L (Pt)	~20 ~20	~80 ~80
$CrPt_3$ → CrPt	<700 ?	Ordering	$CrPt_3$ CrPt	~50 ~50	~50 ~50

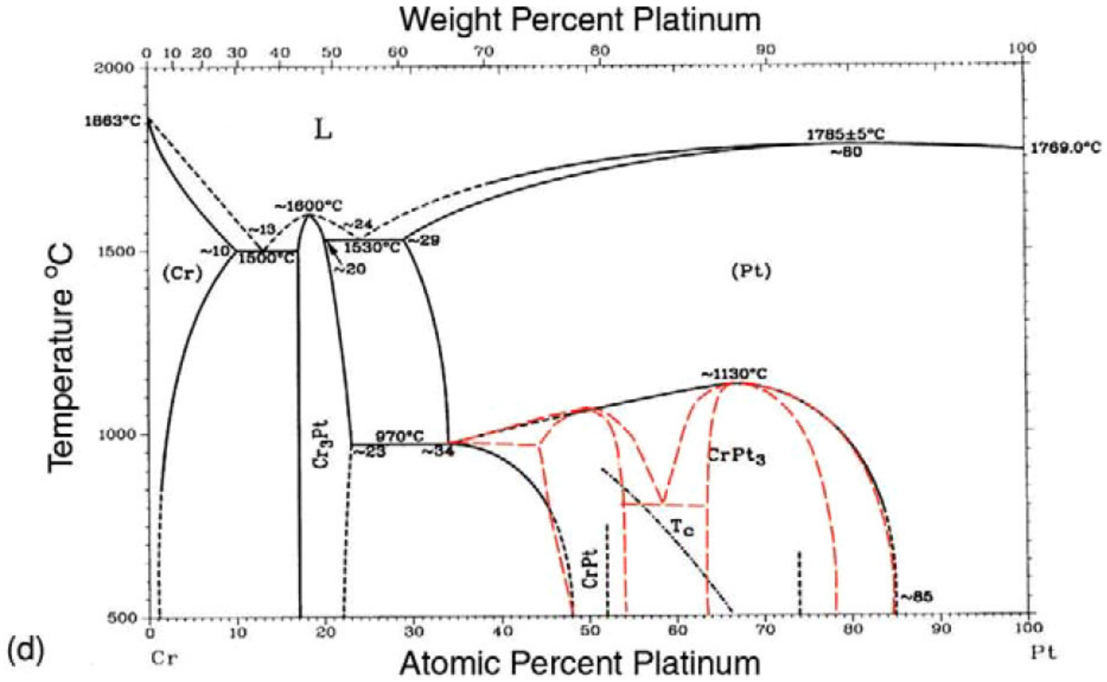

Figure 1.2. Proposed refinement by Zhao et al. [2005Zhao] (dotted lines) of the Cr-Pt phase diagram.

Thermodynamics

Using Miedema's model, a value of ΔH=-36kJ/mol (of atoms) for the enthalpy of formation of CrPt was calculated [1982DeB]. Kuentzler et al. measured low temperature heat capacities in (Pt) [1973Kue, 1974Kue, 1981Kue]. Oikawa et al. calculated the binary Cr-Pt diagram using the CALculation of PHase Diagrams (CALPHAD) technique (Figure 1.2, [2001Oik]). In this calculation, thermodynamic properties of the fcc solid solution phase measured by Scherdweger et al. and Kay et al. [1965Sch, 1970 Kay] were used, while the lattice stability parameters of the pure elements were taken from Dinsdale [1991Din]. Note that Cr_3Pt was not modelled by [2001Oik]. Glatzel et al. [2003Gla] also calculated a diagram, using data from [2001Oik], but included $CrPt_3$ (Figure 1.4) [2003Gla]. However, it had a limited stability range and no provision had been made for the proposed eutectoid reaction at ~970°C. When presented at *Calphad XXXIII* [2004Süs2] it was heavily criticised.

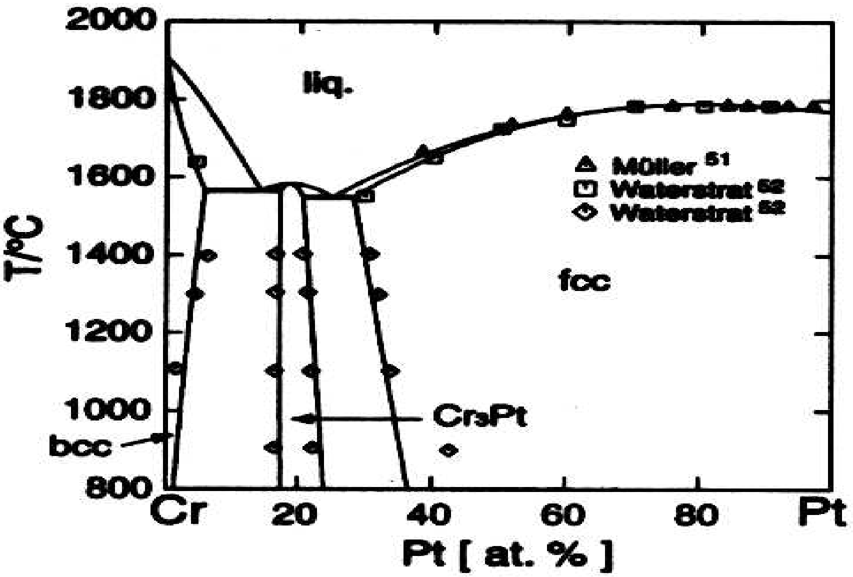

Figure 1.3. Calculated binary Cr-Pt equilibrium phase diagram [2001Oik].

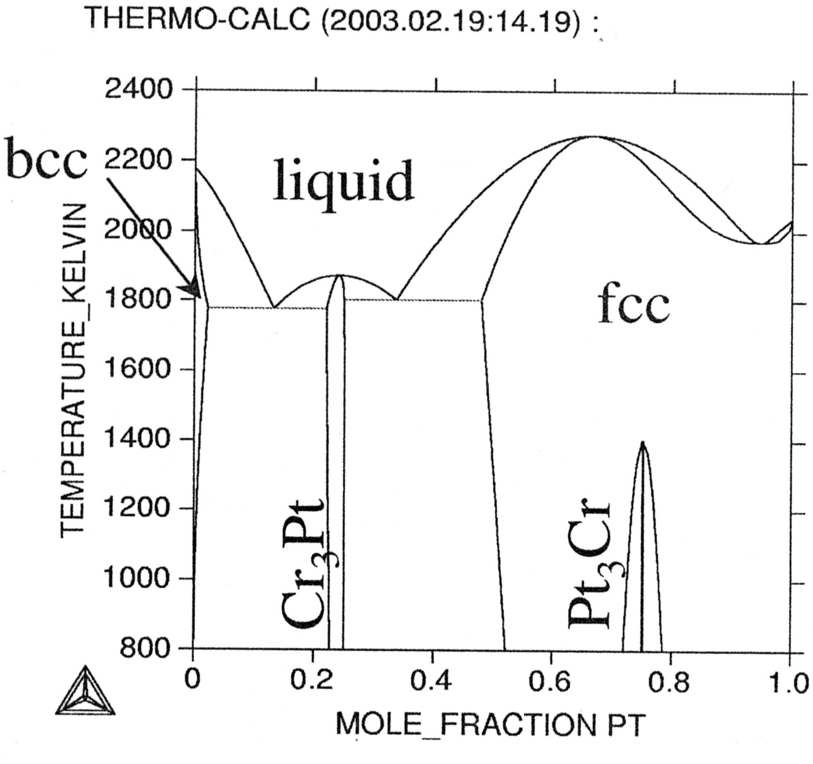

Figure 1.4. Calculated binary Cr-Pt equilibrium phase diagram [2003Gla].

Miscellaneous

Small additions of Pt increase the Néel temperature of pure Cr from 311.5K to 440K (at 0.6 at.% Pt) [1980But], 583 K at 2 at.% Pt [1968Kus], and 460K at 5 at.% Pt [1979Ole]. Disordered (Pt) is paramagnetic, while $CrPt_3$ shows strong spontaneous magnetisation [1977Got]. $CrPt_3$ is ferrimagnetic [1963Pic], with maximum magnetisation near stoichiometric composition [1977Got], which then decreases with increasing Cr until it changes to antiferromagnetic behaviour at ~52 at.% Pt [1935Fri, 1968Kus] to that of the CrPt phase which shows no Néel point [1973Bes]. The addition of Cr strongly increases the electrical resistivity of Pt [1888Bar, 1930Mül, 1934Nem, 1935Fri, 1970Nag, 1972Sta].

2.2. The binary Pt-Al phase diagram

The Pt-Al phase diagram is complex and although certain features had been determined reliably, other aspects of this diagram, especially to the Pt-rich end, remain problematic. McAlister and Kahan reviewed the Pt-Al system in 1986 [1986McA] for the Bulletin of Alloy Phase Diagrams [1990Mas]. The assessed phase diagram (Figure 1.5) was based on the work of Huch [1964Huc], Darling [1970Dar], Chattopadhyay [1975Cha, 1976Cha], Bhan [1978Bha] and Piatti [1980Pia].

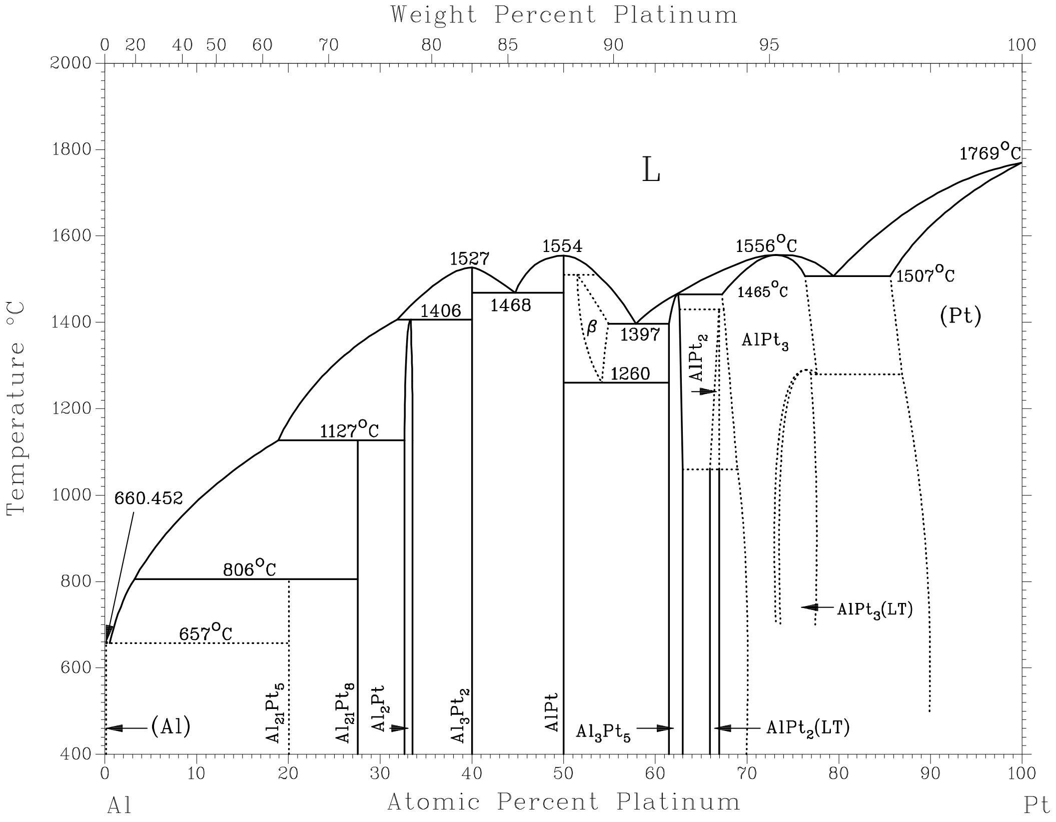

Figure 1.5. Binary Al-Pt equilibrium phase diagram [1990Mas].

The solid phases

Table 1.3 shows the solid phases and their crystal data.

Table 1.3. Al-Pt crystal structure data [1990Mas].

Phase	Composition (at.% Pt)	Pearson symbol	Space group	Struktur-Bericht Designation	Prototype
(Al)	0	cF4	Fm3m	A1	Cu
Pt_5Al_{21}	19.2	Cubic			
Pt_8Al_{21}	27	tI116	$I4_1a$		
$PtAl_2$	31.5 – 33.5	cF12	Fm3m	C1	CaF_2
Pt_2Al_3	40	hP5	P3m1		
PtAl	50	cP8	$P2_13$	B20	FeSi
β	~52 - ~56	cP2	Pm3m	B2	CsCl
Pt_5Al_3	~61.5 – 63	oP16	Pbam		Ge_3Rh_5
Pt_2Al	~66 - ~67	oP12	Pnma	C23	$PbCl_2$
Pt_2Al(LT)	~66 - ~67	oP24	Pmma		$GaPt_2$(LT)
Pt_3Al	~67.3 - ~77.7	cP4	Pm3m	$L1_2$	$AuCu_3$

Phase	**Composition (at.% Pt)**	**Pearson symbol**	**Space group**	**Struktur-Bericht Designation**	**Prototype**
Pt_3Al(LT)	~73.5 – 100	tP16	P4/mbm	$D0'_C$ [1986Mis]	$GaPt_3$(LT)
(Pt)	~83.8 – 100	cF4	Fm3m	Al	Cu
Metastable phases					
α′		cF4	Fm3m	A1	Cu
$PtAl_4$	~20				
$PtAl_6$	~14				
ε′					
λ′	10 – 25				

Phase equilibria

Table 1.4 summarises the reactions that occur on cooling in the Pt-Al system.

Table 1.4. Reactions on cooling in the Pt-Al system [1990Mas].

Reaction	**Reaction phase compositions (at.% Pt)**			**Temperature (°C)**	**Reaction type**
$L \rightarrow (Pt) + Pt_3Al$	79.5	76.4	85.7	1507	Eutectic
$PtAl + L \rightarrow \beta$	50	53.7	51.5	1510	Peritectic
$L \rightarrow Al_3Pt_2 + AlPt$	44.7	40	50	1465	Eutectic
$L + Pt_3Al \rightarrow Pt_5Al_3$	62.3	67.3	62.5	1465	Peritectic
$Pt_3Al + Pt_5Al_3 \rightarrow Pt_2Al$	67.5	62.7	67	1430	Peritectoid
$L + Pt_2Al_3 \rightarrow PtAl_2$	31.8	40	33.3	1406	Peritectic
$L \rightarrow \beta + Pt_5Al_3$	55.7	57.9	66.5	1397	Eutectic
$Pt_3Al \rightarrow Pt_3Al$(LT) + (Pt)	77.7	77	87	1280	Eutectoid
$\beta \rightarrow PtAl + Pt_5Al_3$	54.2	50	61.5	1260	Eutectoid
$L + Pt_2Al \rightarrow Pt_8Al_{21}$	18.8	32.6	27.5	1127	Peritectic
$Pt_2Al \rightarrow Pt_2Al$(LT)		67		1060	?
$L + Pt_8Al_{21} \rightarrow Pt_5Al_{21}$	3.1	27.5	19.2	806	Peritectic
$L \rightarrow (Al) + Pt_5Al_{21}$	0.44	0.0	19.2	657	Eutectic
$L \rightarrow (Pt)$		100		1769	Melting
$L \rightarrow Pt_3Al$		73.2		1556	Congruent
$L \rightarrow PtAl$		50		1554	Congruent
$L \rightarrow Pt_2Al_3$		40		1527	Congruent
$Pt_3Al \rightarrow Pt_3Al$(LT)		76.5		1290	Martensitic?
$L \rightarrow Al$		0		660.4	Melting

Pt is practically insoluble in (Al) [1964Huc]. Extrapolation of the eutectic reaction

$$L \rightarrow (Al) + Pt_5Al_{21}$$

at 627 °C by McAlister [1986Mca] places the eutectic composition at 0.44 at. % Pt, which is in agreement with unidirectional solidification experimental work by Piatti [1980Pia].

Pt_5Al_{21} is a complex cubic stoichiometric phase with essentially no solubility. Huch reported a cubic '$PtAl_4$' with ~20 at. % Pt. It was suggested that the phase might actually be of the Pt_5Al_{21} form instead [1964Huc]. Piatti confirmed this suggestion [1980Pia]. Guex also reported a complex cubic phase of either $PtAl_4$ or Pt_5Al_{21} structure [1976Gue]. Schaller reported, without experimental detail, a hexagonal Pt_5Al_{21} phase [1979Sch]. Ellner confirmed a hexagonal phase and called it $PtAl_4$ [1982Ell]. Piatti also reported a hexagonal phase in this composition range, but noted a transformation from hexagonal to cubic phases after treatment at 200 °C at several hours [1980Pia]. Careful analysis by McAlister of thermal arrest data by Huch and Klemm, in conjunction with a Pt_6Al_{21} phase reported at about this composition, confirmed the phase as Pt_5Al_{21} [1986Mca]. $PtAl_4$ and Pt_6Al_{21} have therefore been suggested as metastable phases in the Pt-Al system.

The stoichiometric Pt_8Al_{21} phase at 27.5 at.% Pt has been confirmed by Edshammer [1968Eds] and Ellner [1982Ell] after earlier reports of a $PtAl_3$-like phase by Huch [1964Huc] and Guex [1976Gue]. The structure of Pt_8Al_{21} has not been determined.

The $PtAl_2$ has been reported as a line compound by Guex [1976Gue], while Huch [1964Huc] and Ellner [1982Ell] reported a ~1 at.% solubility range up to 850°C.

Pt_2Al_3 has a structure related to, but not isotypic with, hexagonal Ni_2Al_3 and essentially no solubility range. It was reported by [1976Gue, 1964Huc, 1982Ell].

Experimental evidence of a β-phase existing between 1260 - 1500°C with a solubility range from 51 - 56 at.% Pt has been reported [1975Cha, 1978Bha]. McAlister and Kahan included these observations in their assessment of the Pt-Al system and proposed a peritectic reaction

$$L + PtAl \rightarrow \beta.$$

An eutectoid decomposition

$$\beta \leftrightarrow PtAl + Pt_5Al_3$$

has also been proposed by McAlister [1986Mca] to correspond with a thermal arrest reported by [1964Huc]. Prins et al. observed microstructural evidence of the $L \rightarrow \beta + Pt_5Al_3$ eutectic and $\beta \leftrightarrow PtAl + Pt_5Al_3$ eutectoid reactions in the ternary Pt-Al-Ru system [2003Pri, 2005Pri].

Although a Pt_3Al_2 phase was reported [1964Huc, 1976Gue], subsequent studies have failed to confirm the existence of this phase.

Figure 1.5 shows Pt_5Al_3 having a solubility range 61.5 - 63 at.% Pt, as reported by Ellner and Oya [1987Oya]. In contrast, Pt_5Al_3 was originally reported as a line compound, the doubtful phase Pt_3Al_2 being included [1964Huc, 1976Gue].

Two crystal variants of the Pt_2Al phase have been reported. Although the low temperature form was not observed by all the researchers, and the nature of the reaction is still unknown, it is accepted that this reaction exists at 1060°C. The reaction was observed, more recently, by Biggs [2001Big].

The highest Pt-containing intermetallic phase is Pt_3Al. A martensitic transformation has been reported where cubic ($L1_2$ - ordered fcc) Pt_3Al transforms to a tetragonal $D0'_c$ Pt_3Al during cooling [1986Mis]. The transformation temperature has been reported as a congruent transformation at 1290°C or a eutectoid reaction at 1280°C, while Oya reported it at about 130°C with another (unconfirmed) intermediate transformation at about 340°C (Figure 1.6 [1987Oya]). The $D0'_c$ phase was reported to be extremely unstable. Biggs [2001Big] observed two low temperature reactions at ~130°C and ~320°C, which coincide with the $\gamma' \rightarrow \gamma_1' \rightarrow \gamma_2'$ reactions reported by Oya at 613 and 400K respectively [1986Mis, 1987Oya].

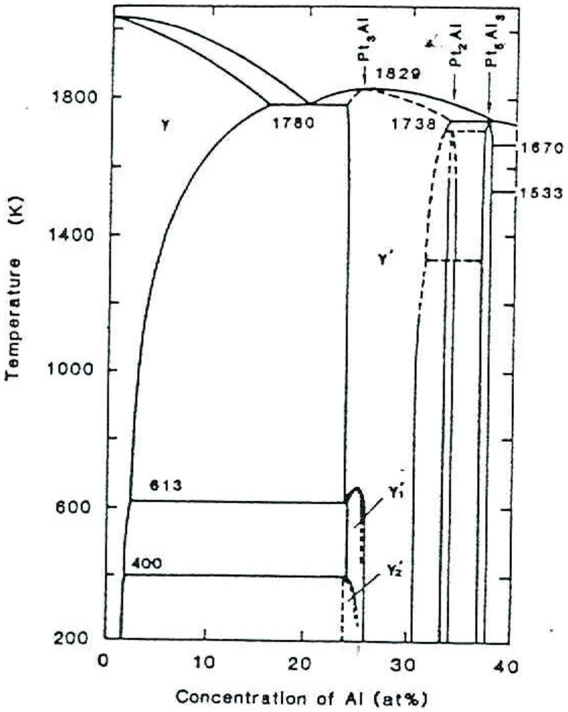

Figure 1.6. Binary Al-Pt equilibrium phase diagram [1987Oya].

(Pt) dissolves ~14 at.% Al at 1510°C [1964Huc, 1970Dar]. Darling suggested a lower solubility of Al in (Pt) at lower temperatures, confirmed as 10 at.% Pt at 1200°C by Bronger and Klemm [1962Bro], and 10 and 5 at.% Pt at 1000 and 300°C respectively [1979Sch].

Thermodynamics

Wu and Jin calculated the Pt-Al phase diagram with the CALPHAD technique [2000Wu]. However, the β and Pt_2Al phases were excluded. They have modeled only the high temperature Pt_3Al phase. Both $PtAl_2$ and Pt_5Al_3 have been modeled as line compounds, making no provision for composition ranges. A recent reassessment by Prins allowed for the introduction of the effects of ordering of the Pt_3Al phase, and the Pt_2Al has also been included [2003Pri, 2004Pri].

The assessed phase diagram by Prins [2004Pri] is given in Figure 1.7. Although both the high and low temperature Pt_3Al phases were modelled, no actual transformation temperature is given in the diagram.

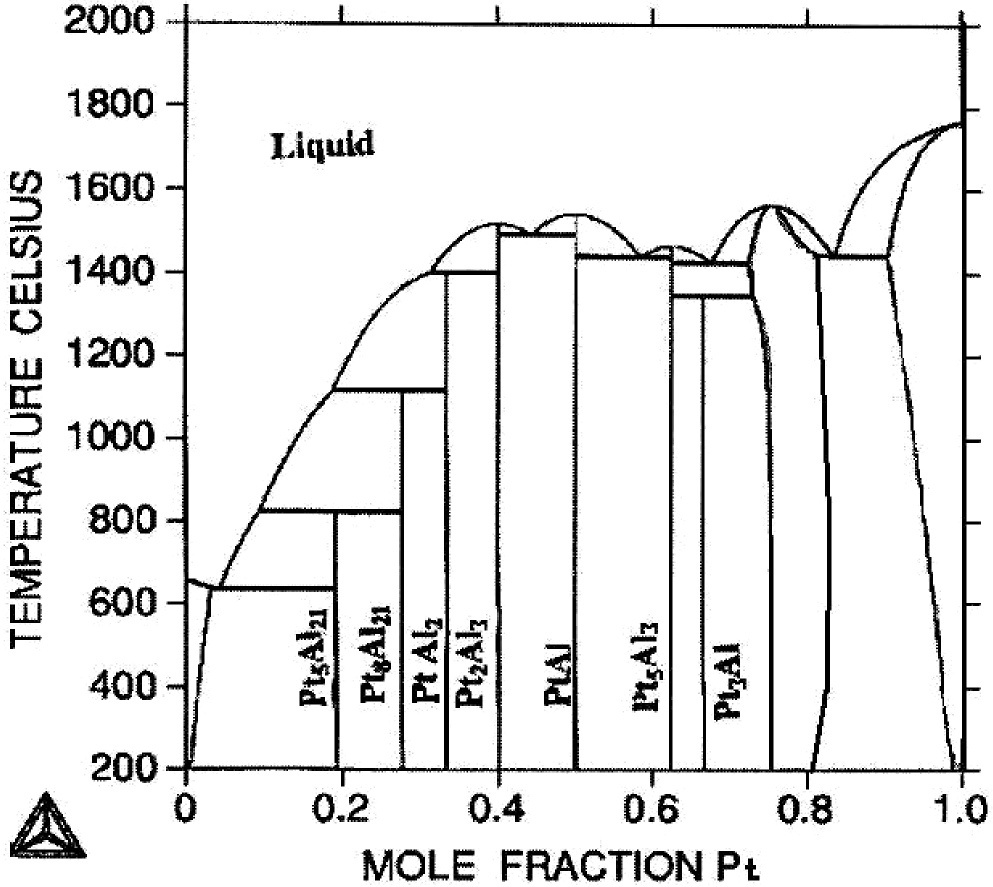

Figure 1.7. Calculated binary Al-Pt equilibrium phase diagram [2002Pri1].

Table 1.5 compares the calculated enthalpies of formation with those determined experimentally.

Table 1.5. Enthalpies of formation for the stable phases (kJ.mol^{-1}) [2004Pri].

Phase	**ΔH$_f$ (experimental)**	**Reference**	**ΔH$_f$ (calculated)**	**Reference**
Pt_5Al_{21}	-57.32	[1968Fer]	-56.83	[2004Pri]
Pt_8Al_{21}	-71.13	[1968Fer]	-81.75	[2004Pri]
$PtAl_2$	-84.00	[1968Fer]	-87.33	[2004Pri]
Pt_2Al_3	-94.98 -79.00 -96.50	[1968Fer] [1988DeB] [1993Mes]	-89.84	[2004Pri]
PtAl	-100.42 -100.00 -82.00	[1968Fer] [1991Jun] [1988DeB]	-67.44 -94.03	[2002Ngo] [2004Pri]
Pt_5Al_3	-90.73	[1998Wol]	-87.21	[2004Pri]

Phase	**ΔH_f (experimental)**	**Reference**	**ΔH_f (calculated)**	**Ref**
Pt_2Al	-88.28	[1998Wol]	-85.28	[2004Pri]
Pt_3Al	-69.87 -63.60 -50.99 -76.00	[1968Fer] [1993Mes] [1988DeB] [1981Wor]	-74.38 -51.67	[2002Ngo] [2004Pri]
Pt_3Al(LT)			-79.10	[2002Ngo]

2.3. The binary Al-Cr phase diagram

Murray reviewed the literature up to 1988 and gave an assessed diagram, as well as a calculated one [1998Mur]. A thermodynamic assessment was also undertaken by Saunders et al. [1986Sau, 1987Sau], Ansara et al. [1998Ans] and Mahdouk et al. [2000Mah]. A calculated diagram was published by Dupin [2001Dup] based on the thermodynamic description by Saunders [1998Sau] based on his earlier work [1987Sau]. Recent thermodynamic work is summarised in Table 1.6. Cornish et al. reviewed the literature up to 2002 [2002Cor2].

Table 1.6. Recent Investigations on the Al–Cr system.

Reference	**Experimental Technique**	**Temperature/ Composition/ Phase range studied**
[1989Ell]	Metallography, XRD	30-42, 75-85 at.% Cr
[1992Cos]	DTA, metallography, diffusion couples, electron microprobe	5.4-61 at.% Cr
[1995Aud]	DTA, TEM	17, 20, 25 at.% Cr
[1996Lee]	TEM, XRD	10, 15, 48 at.% Cr
[1999Hel]	XRD	58.4, 60.9, 64.8, 67.5 at.% Cr
[2000Mah]	DTA, XRD, EPMA, Direct reaction calorimetry	13, 16, 19.5, 31, 39 at.% Cr

Solid Phases

Table 1.7 shows the solid phases. Cr_2Al_{13} is considered the more correct composition for $CrAl_7$ [1998Mur]. Similarly, $CrAl_5$ has been suggested for Cr_2Al_{11}. Both Cr_2Al_{11} (decomposing at 785°C [2000Mah]) and $CrAl_4$ have been reported as showing metastable behaviour [1998Mur].

Costa Neto et al. [1992Cos] reported no Cr_2Al_{11} in either as-cast or annealed samples although the composition did occur in diffusion studies, as well as that of 25.6 at.%. [1992Cos]. Conversely, Audier et al. [1995Aud] found a peak corresponding to the peritectic formation of Cr_2Al_{11} [1995Aud]. It was suggested that Cr_2Al_{11} formed in the solid state during slow cooling, but that nucleation is difficult [1995Aud].

An icosahedral phase has formed on rapid solidification in as-spun-ribbons comprising 8-13 at.% Cr [1985Dun, 1986Ben, 1988Zha] and has the composition ~20 at.% Cr, $\iota CrAl_4$ [1986Lil]. Zhang et al. established the orientation relationship between $\iota CrAl_4$ and $CrAl_7$ [1988Zha]. It was shown that the $\mu CrAl_4$ had similar icosahedral clusters to $CrAl_7$, as well as a relationship with Cr_2Al_{11} [1995Aud]. Wen et al. and Selke et al. [1992Wen, 1994Sel] demonstrated the relationship between $CrAl_7$ and the $CrAl_4$ variants. Li et al. demonstrated icosahedral structures in $\varepsilon CrAl_4$ [1997Li], [1998Li] showed its structural relationship to the Al–Cr–Ni κ phase [1998Li], and Uchida et al. [2000Uch] developed a new stacking motif to demonstrate the relationship between these and other phases [2000Uch].

A high-temperature structure has been found referred to as βCr_5Al_8, and a low temperature structure as αCr_5Al_8, with the structure change between 1170-1200°C depending on composition. There are also three temperature-dependent structures of the Cr_4Al_9 phase, but it was reported that the Cr_4Al_9 and Cr_5Al_8 phases were contiguous [2000Mah], with the contiguity occurring within the Al–Cr–Fe ternary [2000Sub]. Ellner et al. and Brown at al. [1989Ell, 1992Bra] also found a single phase by liquid quenching. There is general acknowledgement that the structure of the phases is closely related.

Ordering of (Cr) to B2 just above its eutectoid decomposition was reported [1963Koe, 1999Hel].

Table 1.7. Solid phases of Al-Cr.

Phase/ Temperature Range (°C)	**Pearson Symbol/ Space Group/ Strukturbericht/ Prototype**	**Lattice Parameters (pm)**	**Comments**
(βAl)	*hP*2 $P6_3/mmc$ --- Mg	a = 269.3 c = 439.8	at 25°C, 20.5 GPa [Mas2]
(Al) <660.452	*cF*4 $Fm\bar{3}m$ *A*1 Cu	a = 404.96	at 25°C [Mas2]
(α'Cr)	*tI*2 *I*4/*mmm* --- α´Cr	a = 288.2 c = 288.7	at 25°C, HP [Mas2]
(αCr) <1863	*cI*2 $Im\bar{3}m$ --- W	a = 288.48	at 25°C [Mas2]
Cr_2Al_{13} ($CrAl_7$) 790-200	*mC*104 *C*2/*m* --- V_7Al_{45}	a = 2519.6 b = 757.4 c = 1094.9 β = 128.7°	[1975Ohn]
Cr_2Al_{11} ($CrAl_5$) 940-200	*mP*48 *P*2 $CrAl_5$ *C*2/*c*	a = 1288.0 b = 765.2 c = 1063.9 β = 128.4°	[1975Ohn]
Cr_2Al_{11} ($CrAl_5$) 940-200	--- *Cmcm* ---	a = 1240 b = 3460 c = 2020 β = 122.3°	[1995Aud]
$CrAl_4$ 1030-200	*mP*180 *P*2/m --- $CrAl_4$	a = 871.6 b = 2394.6 c = 1638.6 β = 119.33°	[1975Ohn]
μ$CrAl_4$	$P6_3/mmc$ --- μ-$MnAl_4$	a = 2000 b = 2000 c = 2470	[1992Wen]
ε$CrAl_4$	*oC*584 *Cmcm* ---	a = 1252.1 b = 3470.5 c = 2022.3 a = 3460 b = 2000 c = 1260	Single crystal [1997Li, 1998Li] [1992Wen]
ι$CrAl_4$	---		Icosahedral [1986Lil]
γCr_4Al_9 1170-1060	**---**		[1963Koe]

Phase/ Temperature Range (°C)	**Pearson Symbol/ Space Group/ Strukturbericht/ Prototype**	**Lattice Parameters (pm)**	**Comments**
βCr_4Al_9 ~1060-200	---		[1963Koe]
αC_4Al_9 ~700-200	$cI52$ $I\bar{4}3m$ --- Cr_4Al_9	$a = 912.3$	[1963Koe]
βCr_5Al_8 1350-250	$cI52$ $I43m$ --- Cu_5Zn_8	$a = 904.7$ to 910.4	30 to 42 at .% Cr. Quenched from liquid [1989Ell]
αCr_5Al_8 ~1150-200	$hR26$ $R\bar{3}m$ $D8_{10}$ Cr_5Al_8	$a = 1272.8$ $c = 794.2$ $a = 1281.3$ $c = 795.1$	[1977Bra] [1989Ell]
Cr_2Al 910-200	$tI6$ $I4/mmm$ $A2$ $MoSi_2$	$a = 300.5$ to 302.8 $c = 864.9$ to 875.5	298 to 1126 K [1989Ell]
X 350-200	---		[1981Den, 1981Van]

Phase Equilibria

Table 1.8 and Figure 1.8 show the phase equilibria. The reaction between (Al) and $CrAl_7$ has usually been reported as peritectic, although Costa Neto et al. and Mahdouk et al. [1992Cos, 2000Mah] reported it as eutectic in nature. However, as Cr lies between transition metals which have eutectic reactions (Mn–Ni) and those which have peritectic reactions (Ti–V) [1990Mas], the reaction will obviously be very sensitive to impurities. The purities of the Al and Cr of [1992Cos] were 99.9% and 99.5% respectively, whereas those of Mahdouk [2000Mah] were both 99.5%. Thus, the higher impurity could have lowered the reaction temperature, especially as the work with the highest impurity has the lowest reaction temperature, and Al–Cr systems with ternary additions are often eutectic. Thus, the more commonly reported peritectic reaction [1998Mur] is used, which includes earlier studies using 99.99% purity elements.

The eutectoid decomposition of Cr_2Al_{11} was reported and it was stated that it should not have been effected by the impurities, although 99.5% starting materials were used [2000Mah]. However, the amorphous phase at 460°C contradicts this [1996Lee].

Shao et al. [2000Sha1, 2000Sha2] reported the ω phase (as in Ti alloys) in the Cr_2Al structure in melt-spun alloys.

Most authors reported that more work needs to be done on the system.

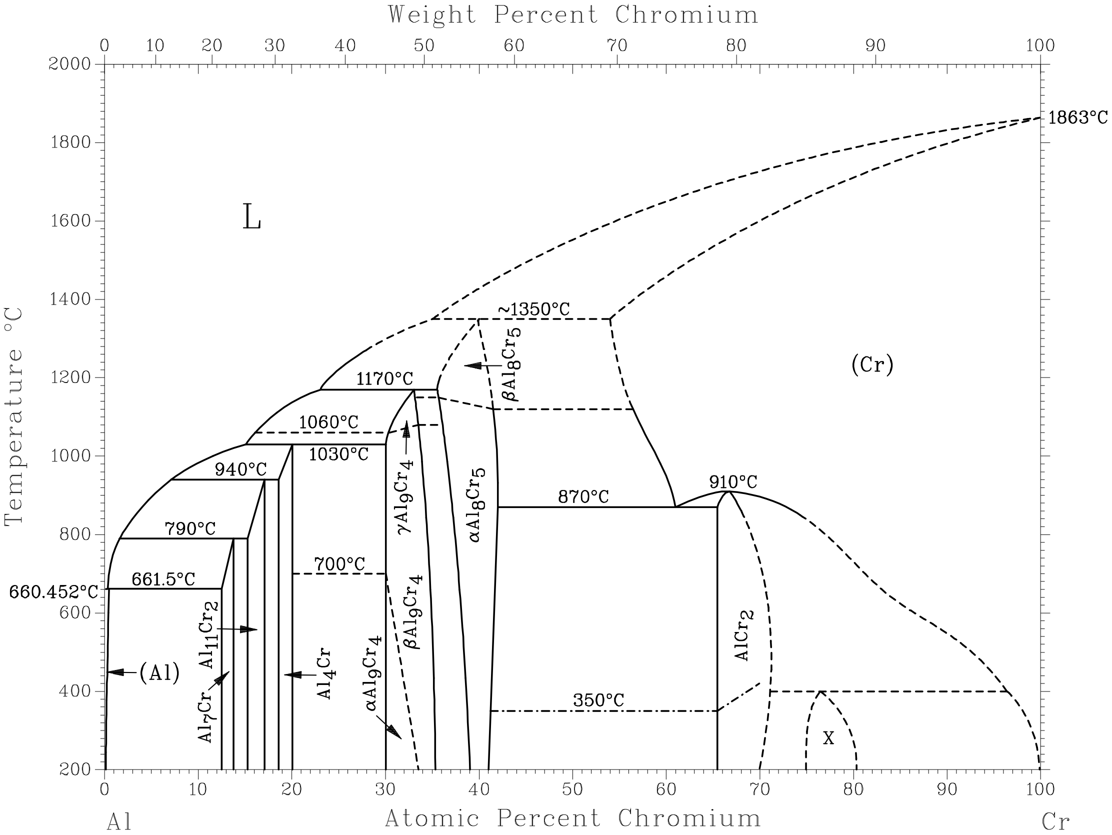

Figure 1.8. Binary Al-Cr equilibrium phase diagram [1990Mas].

Table 1.8. Invariant equilibria of Al-Cr.

Reaction	**T (°C)**	**Type**	**Phase**	**Composition (at.%)**	
				Al	**Cr**
$L+Cr_2Al_{13}\rightarrow(Al)$	661.5	Peritectic	L Cr_2Al_{13} (Al)	99.8 88 99.65	0.2 12 0.35
$L+Cr_2Al_{11}\rightarrow Cr_2Al_{13}$	790	Peritectic	L Cr_2Al_{11} Cr_2Al_{13}	98.9 84.8 86.8	1.1 15.2 13.2
$L+ CrAl_4\rightarrow Cr_2Al_{11}$	940	Peritectic	L $CrAl_4$ Cr_2Al_{11}	93.5 81.5 83.0	6.5 18.5 17.0
$L+\beta Cr_4Al_9\rightarrow CrAl_4$	1030	Peritectic	L βCr_4Al_9 $CrAl_4$	85.5 70 80.0	14.5 30 20.0
$L+\beta Cr_5Al_8\rightarrow\gamma Cr_4Al_9$	1170	Peritectic	L βCr_5Al_8 γCr_4Al_9	77.5 64.5 66.7	22.5 35.5 33.3
$L+(Cr)\rightarrow\beta Cr_5Al_8$	~1350	Peritectic	L (Cr) βCr_5Al_8	~65 ~46 ~60.5	~35 ~54 ~39.5
$(Cr)\rightarrow Cr_5Al_8+Cr_2Al$	870	Eutectoid	(Cr) Cr_5Al_8 Cr_2Al	35 58.0 34.5	65 42.0 65.5
$Cr_2Al_{11}\rightarrow Cr_2Al_{13}+CrAl_4$	785	Eutectoid	Cr_2Al_{11} Cr_2Al_{13} $CrAl_4$	84 86.8 81.5	16 13.2 18.5
$(Cr)\rightarrow Cr_2Al$	910	Congruent	(Cr) Cr_2Al	33.3 33.3	66.7 66.7
$(Cr)+Cr_2Al\rightarrow X$	350	Congruent	(Cr) Cr_2Al X	~4 ~29 ~24	~94 ~71 ~76

Thermodynamics

Table 1.9 gives the thermodynamic properties of the solution and compound phases after Saunders et al. [1987Sau, 1998Sau]. Thermodynamic work after 1988 is given in Table 1.6. Thermodynamic properties of solid Al–Cr alloys have been measured using EMF [1971Sam] and isopiestic techniques [1968Joh]. The enthalpy of formation for the Al–Cr intermetallic phases was measured using calorimetry [1960Kub, 1994Mes, 2000Mah, 2001Mes].

The partial molar enthalpy of dissolution of Cr in liquid Al at infinite dilution at 800°C was derived as 50.6 ± 0.83 $kJ\cdot mol^{-1}$ [1994Zub], which was in good agreement with Miedema

[1977Mie]. Partial and integral mixing enthalpies were also directly determined at 1647°C in the composition range 0-30 at.% Cr [1990Sud]. The partial and the integral enthalpies of mixing of liquid Al–Cr binary alloys have been determined by high temperature mixing isoperibolic calorimetry at 1450°C [2002Sal].

The solvus was determined using activation data [1994Dia], but disagreed with published values above 500°C, and difficulty in reaching equilibrium was experienced below 430°C. Evaporation experiments were undertaken [1990Ter].

In all the calculated phase diagrams all the intermetallic phases are modelled as stoichiometric compounds [1998Sau, 2001Dup].

Table 1.9. Thermodynamic Data of Reaction or Transformation [2002Cor2].

Reaction or Transformation	**Temperature (°C)**	**Quantity, per mol of atoms (kJ, mol, K)**	**Comments**
1/15{2Cr(s) + 13Al(s) → Cr_2Al_{13}(s)}	710 -	ΔH = -0.893±0.04 ΔH = -0.86±0.03	[2000Mah] direct reaction calorimetry [1993Cho] Ion beam mixing
1/13{2Cr(s) + 11Al(s) → Cr_2Al_{11}(s)}	843 -	ΔH = -0.88±0.03 ΔH = -1.15±0.035	[2000Mah] direct reaction calorimetry [1993Cho] Ion beam mixing
1/5{Cr(s) + 4Al(s) → $CrAl_4$(s)}	921 -	ΔH = -3.34±0.16 ΔH = -3.42±0.08	[2000Mah] direct reaction calorimetry [1993Cho] Ion beam mixing
1/13{4Cr(s) + 9Al(s) → Cr_4Al_9(s)}	940 -	ΔH = -1.37±0.04 ΔH = -1.22±0.02	[2000Mah] direct reaction calorimetry [1993Cho] Ion beam mixing
1/13{5Cr(s) + 8Al(s) → $Cr_5Al_8(\alpha)$}	1010 -	ΔH = -1.36±0.03 ΔH = -1.15	[2000Mah] direct reaction calorimetry [1993Cho] Ion beam mixing
1/13{5Cr(s) + 8Al(s) → $Cr_5Al_8(\beta)$}	1203 1200±2	ΔH = -1.36±0.04 ΔH = -1.3±0.14	[2000Mah] direct reaction calorimetry [1994Mes, 2001Mes] direct reaction calorimetry
1/3{2Cr(s) + Al(s) → Cr_2Al(s)}	-	ΔH = -3.6	[1993Cho] Ion beam mixing

Reaction or Transformation	Temperature (°C)	Quantity, per mol of atoms (kJ, mol, K)	Comments
Cr(s, 25°C) + L (n = ∞) → L (x_{Al} = 1)	800 1450	ΔH = -50.6±0.83 ΔH = -33.1±0.3	[1994Zub] drop calorimetry, infinite dilution [2002Sal] isoperibolic mixing calorimetry, infinite dilution
Cr(s, 25°C) + L (n = ∞) → L (x_{Al} = 0.9)	1450 1647	ΔH = -2.7 ΔH = -2.9	[2002Sal] isoperibolic mixing calorimetry [1990Sud] drop calorimetry
Cr(s, 25°C) + L (n = ∞) → L (x_{Al} = 0.8)	1450 1647	ΔH = -4.5 ΔH = -5.0	[2002Sal] isoperibolic mixing calorimetry [1990Sud] drop calorimetry
Cr(s, 25°C) + L (n = ∞) → L (x_{Al} = 0.7)	1450 1647	ΔH = -6.9 ΔH = -6.6	[2002Sal] isoperibolic mixing calorimetry [1990Sud] drop calorimetry
Cr(s, 25°C) + L (n = ∞) → L (x_{Al} = 0.6)	1450	ΔH = -7.9	[2002Sal] isoperibolic mixing calorimetry

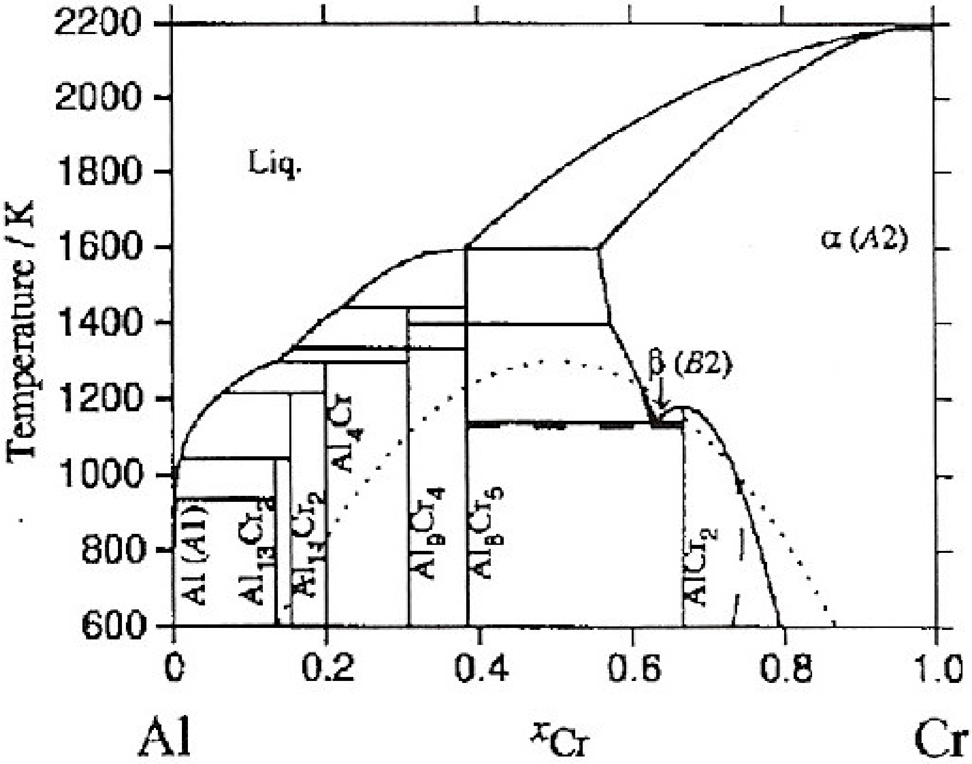

Figure 1.9. Calculated binary phase diagram of Al-Cr [2001Dup].

Materials Properties and Applications

Small amounts of Cr are used to prevent recrystallisation and grain growth, and so increase the strength of aluminium alloys. However, the amounts must not let coarse $CrAl_7$ form. Al and Cr are also important components in Ni-based superalloys.

Miscellaneous

Baran et al. reported the minimum in the magnetic phase diagram to lie between 1.7 and 2.0 at.% Al [1992Bar], rather than their earlier values, and the Néel temperature to be between 100 and 140 K.

Structures and their mechanical properties were studied by [1989Sok, 1994Abr].

2.4. The ternary Pt-Al-Cr system

The partial ternary isothermal section of the Pt-Al-Cr system at 1350°C as determined by Hill is shown in Figure 1.10 [2001Hil4]. The Pt_3Al phase field has been significantly increased by the addition of Cr compared to its width in the binary system. The single-phase ~Pt_3Al and (Pt) phases are shown, but their phase boundaries were not accurately determined above 30 at.% Cr because it was of no interest to that particular investigation.

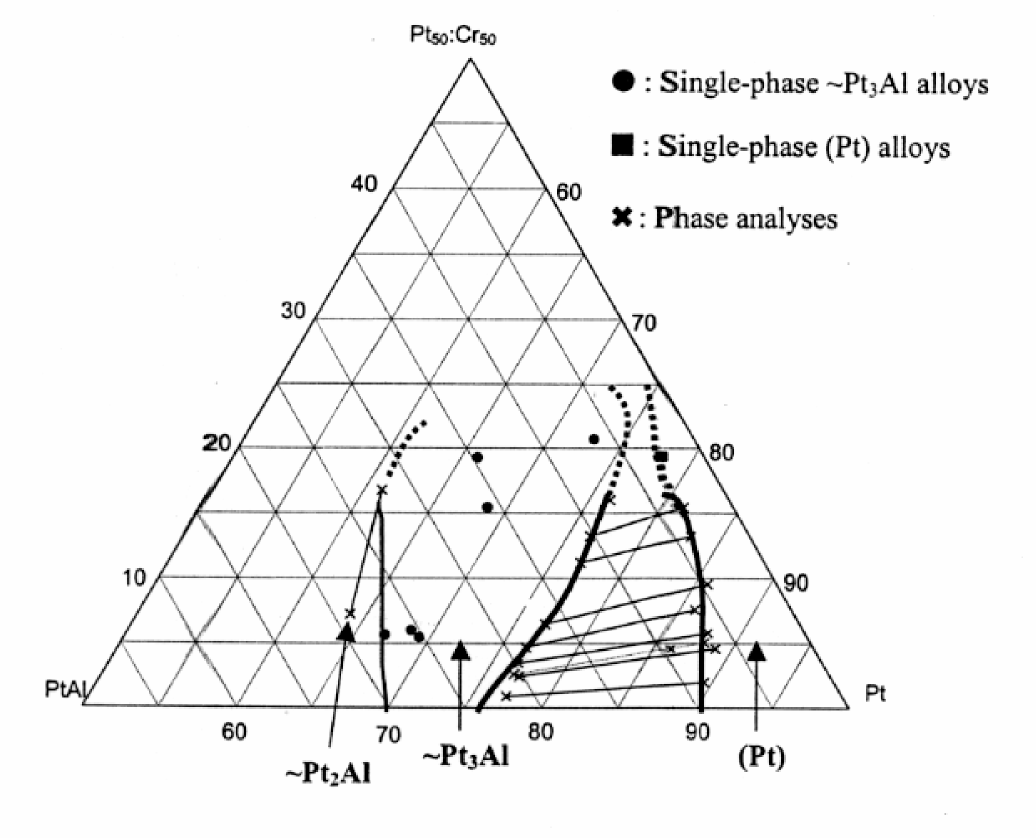

Figure 1.10. Partial isothermal section of the Pt-Al-Cr system at 1350℃ [2001Hil4].